https://doi.org/10.22226/2410-3535-2022-4-457-462

Effect of hot working on the microstructure and tensile properties of a novel PM Re-bearing nickel base superalloy

Sh. Kh. Mukhtarov[†,1], D. A. Karyagin[2], A. V. Logunov[1], A. A. Ganeev[1],
R. I. Zainullin[1], R. V. Shakhov[1], V. M. Imayev[1]

[†]shamilm@imsp.ru

[1]Institute for Metals Superplasticity Problems, RAS, Ufa, 450001, Russia
[2]CMK, Stupino, Moscow Region, 142800, Russia

The work is devoted to study of an experimental PM nickel-based superalloy Ni-16(Al, Ti, Nb, Ta)-30(Cr, Co, Mo, Hf, W, Re) (wt.%). The initial as-HIP'ed material was prepared as cylinders with a size of ∅100 × 200 mm. The hot workability of the superalloy was evaluated by compression tests of small samples under isothermal conditions. The tests were performed at temperatures of 1150 –1240°C with a strain rate of $\dot{\varepsilon}=10^{-4}-10^{-1}$ s^{-1}. Some samples were subjected to preliminary homogenization annealing. Examination of the deformed samples by SEM made it possible to define the hot working conditions providing development of recrystallization processes and formation of a uniform fine-grained structure. It was established that preliminary homogenization of as-HIP'ed material followed by fractional forging with intermediate recrystallization annealings in the temperature range of $(T_s-40)-(T_s-15)$, where T_s is the γ' solvus temperature, provided a uniform development of recrystallization. The obtained forgings were subjected to ageing or solid solution treatment and ageing. In the fine-grained condition obtained by hot working and heat treatment, the material exhibited tensile properties comparable to the best properties achievable in disc nickel-based superalloys.

Keywords: nickel-based superalloy, powder metallurgy, microstructure, hot working, heat treatment, tensile properties.

1. Introduction

Improving the energy efficiency of gas turbine engines (GTE) and similar energy-conversion systems is dependent on the development of novel advanced materials with enhanced mechanical properties. In particular, increasing demands are being placed on nickel-based superalloys, which are widely used for manufacturing of rotary engine parts such as turbine discs in GTE [1]. For this purpose, novel heavily alloyed disc superalloys with a higher content of the γ'(Ni_3Al) forming elements are being designed. In the recently designed powder metallurgy (PM) superalloy the content of (Al + Ti + Nb + Ta) is 16.8 at.% and the ratio (Ti + Nb + Ta)/Al (in at.%) is 0.92, which indicates a significant solid solution hardening of the γ' phase. The γ matrix chemistry was adjusted through a balance between the solid solution elements including refractory rhenium taking into account the prevention of the formation of topologically close-packed (TCP) phases. Note that rhenium as an alloying element in nickel-based superalloys was typically doped in single-crystal superalloys [2 – 5] and only recently has been used for polycrystalline nickel-based superalloys [6 –10]. It is well known that rhenium is one of the most effective solid solution elements that reduces the dislocation mobility in the vicinity of the interphase γ/γ' boundaries, decreases the diffusivity in the matrix γ phase and increases the phase and microstructure stability during long-term exposure at elevated temperatures [11,12]. Therefore, rhenium is known to increase significantly the creep rupture life in the case of single-crystal superalloys [2]. The positive influence of rhenium on mechanical properties has recently also been demonstrated in a polycrystalline nickel-based superalloy [13,14].

The processing routes used for manufacturing of discs made of heavily alloyed nickel-based superalloys are as follows:

i) ingot manufacturing – hot pressing – hot forging [15];

ii) ingot manufacturing – spraying and preparation of powder – hot isostatic pressing (HIP) [16,17];

iii) ingot manufacturing – spraying and preparation of powder – HIP – isothermal forging (gatorizing process) [18];

iv) ingot – spraying and preparation of powder – HIP – hot quasi-isothermal forging [19, 20].

All processing routes are aimed at achieving a certain geometry of the part and a tailored microstructure that provides the required mechanical properties. In addition, the processing route is selected based on the available equipment. For production of large-scale discs for GTE with a homogeneous and refined structure the processing routes ii-iv using the PM material seem to be the most reasonable. This is because the PM material does not suffer from a strong dendritic segregation typically observed in heavily alloyed nickel-based superalloys and has a relatively fine-grained structure already in the as-HIPed condition. To additionally

improve the mechanical properties of the as-HIPed material it makes sense to apply the hot working [21–23]. The aim of the present work is to study the effect of the hot working on the microstructure and tensile properties of a novel heavily alloyed PM nickel-based superalloy with a high content of the γ'(Ni_3Al) forming elements.

2. Materials and experimental

The nominal chemical composition of the PM superalloy is Ni-16(Al, Ti, Nb, Ta)-30(Cr, Co, Mo, Hf, W, Re) (wt.%). The initial as-HIP'ed material was prepared as cylinders with a size of ∅100 × 200 mm. The alloy composition measured by energy dispersive X-Ray (EDS) analysis was very close to the nominal composition. The γ' solvus temperature (T_s) defined by quenching experiments from temperatures 1200–1250°C was found to be $T_s \approx 1240 \pm 5$°C. Homogenization annealing of the as-HIP'ed material was performed at T=1220°C for 15 h. The cylindrical samples of ∅8 × 12 mm for compression tests and the billets of ∅37 × 50 mm for hot working experiments were cut from the as-HIP'ed and the as-HIP'ed and homogenized materials. The compression tests were carried out in the temperature range of T=1150–1240°C with an initial strain rate of $\dot{\varepsilon}=10^{-4}$–$10^{-1}$ s^{-1} to a strain of ε = 65–70% The true stress-strain curves were drawn taking into account a graduate increase in the cross section of the compressed samples during deformation. The results of compression tests were used for hot working of the billets. The billets were subjected to fractional forging in a can made of a stainless steel under quasi-isothermal conditions with intermediate recrystallization annealings in the temperature range of $(T_s-40)-(T_s-15)$. The hot worked workpieces were subjected to solid solution heat treatment at $(T_s-40)-(T_s-30)$ (2 h) followed by cooling in air and ageing or only to ageing that provided partial dissolution of the primary γ' phase while maintaining a fine-grained structure ($d \leq 10$–15 μm). The ageing treatment was carried out at T = 850°C (10 h) and 750°C (50 h).

The hot worked workpieces were cut along their diameters and the cross sections were used to prepare the macrostructures by mechanical polishing and etching. Microstructure examination was carried out for the cross sections of the deformed samples and billets using scanning electron microscopy (Mira-3 Tescan) in the back-scattering electron (BSE) mode. The BSE images were used to evaluate the sizes of γ grains, secondary γ' and carbide particles and the volume fraction of the γ' phase. Electron backscatter diffraction (EBSD) analysis was performed with a scan-step size of 0.5 μm taking into consideration central parts of the deformed samples and billets. EBSD analysis was used to evaluate the sizes of coarse γ grains and primary γ' as well as the fraction of high-angle grain/interphase boundaries. EBSD analysis was conducted using the CHANNEL 5 processing software. The grain/interphase boundaries having misorientation angle less than 2° were excluded from the consideration taking into account the measurement accuracy. The grain/interphase boundaries were assumed as high-angle ones if their misorientation angle was more than 15°.

The hot worked workpieces were used to prepare the flat specimens with a gage section of 10 × 3 × 2 mm for tensile testing. The tensile tests were carried out at 20 and 750°C. Before testing, the tensile specimens were mechanically polished.

3. Results and discussion

3.1. Initial microstructures

Figure 1 shows the BSE images of the superalloy in the initial as-HIP'ed condition. The microstructure is homogeneous with a mean γ grain size of $d \approx 27$ μm (Fig. 1a, b). Primary γ' phase with a size of 3–20 μm are mainly located along γ grain boundaries (Fig. 1b). The secondary γ' phase with a size of 0.2–1.5 μm have an irregular shape typical of nickel-based superalloys after long-term tempering at subsolvus temperatures followed by slow cooling (Fig. 1c). The volume fraction of the γ' phase determined using the BSE images is about 75%. Bright carbide particles have the size of 1–8 μm, their volume fraction was not more than 1% (Fig. 1a, b). Dendritic segregation in the form of γ + γ' eutectic colonies within γ grains was sometimes detected in the microstructure (Fig. 1d). It was obviously inherited from the initial powder granules. In the as-HIP'ed condition some porosity was observed, the volume fraction of the pores was less than 0.5%.

3.2. Compression tests and microstructure examination

Fig. 2 shows the true stress-strain curves obtained as a result of compression tests of samples in the initial as-HIP'ed condition at T=1150–1240°C with an initial strain rate of $\dot{\varepsilon}=10^{-3}$ s^{-1} (a), at T=1175–1225°C with an initial strain rate of $\dot{\varepsilon}=10^{-2}$ s^{-1} (b), and at T=1225°C with an initial strain rate of $\dot{\varepsilon}=10^{-4}$, 10^{-3} and 10^{-2} s^{-1} (after compression at 1225°C with a strain rate of 10^{-1} s^{-1} the sample was completely destroyed). All samples were deformed with surface cracks on the side surfaces of samples. With increasing the test temperature and decreasing the strain rate the flow stress decreases (Fig. 2). All curves look similar. The flow stress values first increase reaching maxima at a strain of 2–4% then decrease up to the middle strain values (10–30%) and then increase again. Most likely, the strange dependences of the flow stress on strain are associated with the formation of cracks on the side surfaces and in the interior of samples. The latter can be caused by pores and dendritic segregation within some grains, which were observed in the initial material.

Microstructure examination confirmed the formation of microcracks along grain/interphase boundaries in the deformed samples. Figure 3 represents the BSE images obtained from the central parts of the cross sections of samples in the initial as-HIP'ed condition deformed at T=1200, 1225 and 1240°C with a strain rate of $\dot{\varepsilon}=10^{-3}$ s^{-1}. The hot compression led to the localized development of recrystallization in the middle part of the deformed samples and the formation of microcracks along grain/interphase boundaries. The microcracks looking like dark dots and lines along boundaries were especially noticeable after compression at T=1240°C (Fig. 3c).

By way of illustration, Fig. 4 shows the EBSD map and the corresponding misorientation-angle distributions for

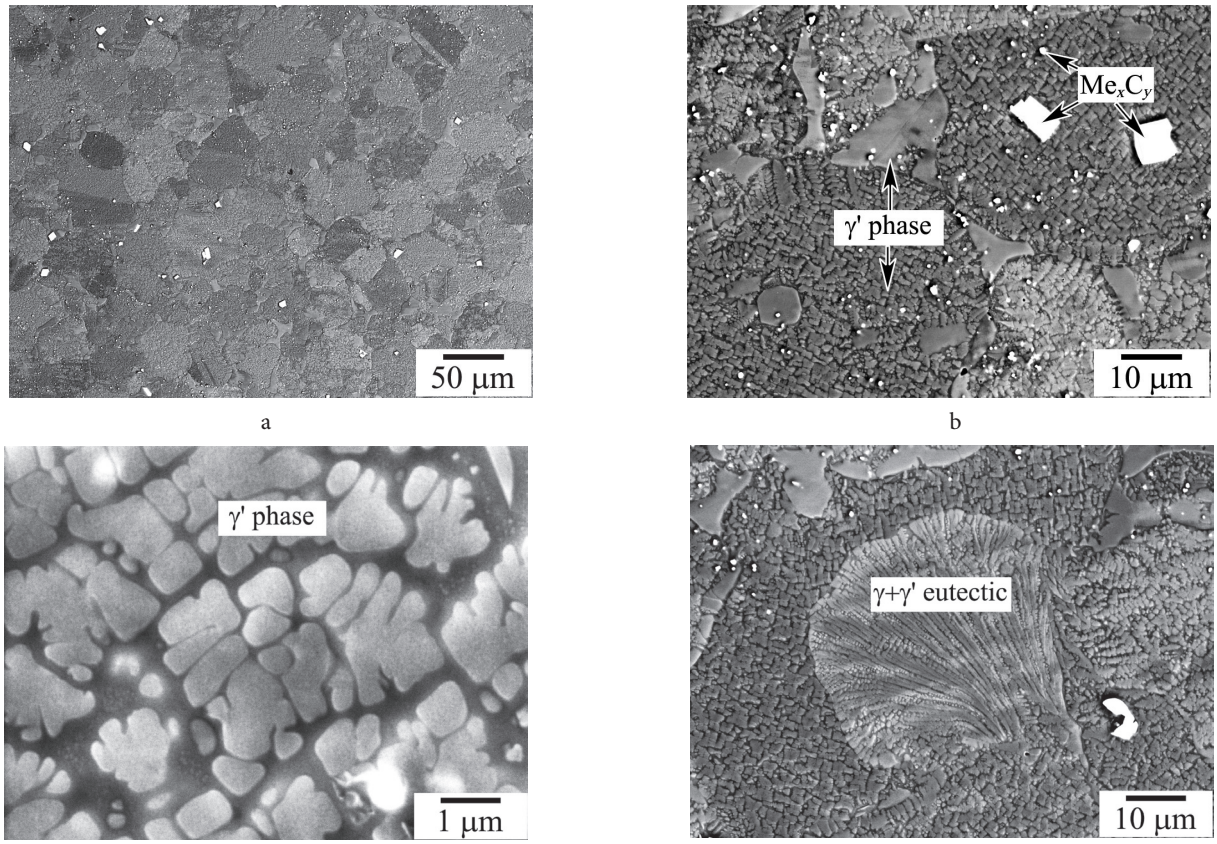

Fig. 1. BSE images of the PM Ni-16(Al, Ti, Nb, Ta)-30(Cr, Co, Mo, Hf, W, Re) superalloy in the as-HIP'ed condition at different magnifications.

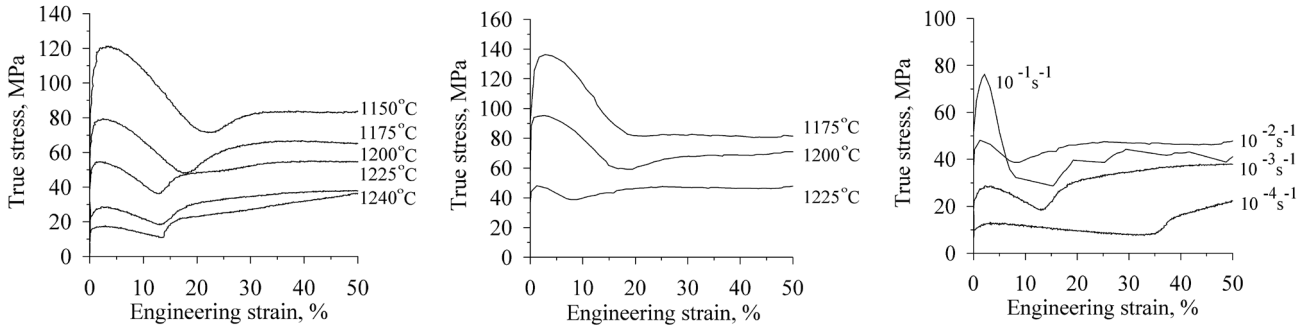

Fig. 2. The true stress-strain curves obtained as a result of compression tests: T=1150–1240°C, $\dot{\varepsilon}=10^{-3}$ s^{-1} (a), T=1175–1225°C, $\dot{\varepsilon}=10^{-2}$ s^{-1} (b), T=1225°C, $\dot{\varepsilon}=10^{-4}$–$10^{-1}$ s^{-1} (c).

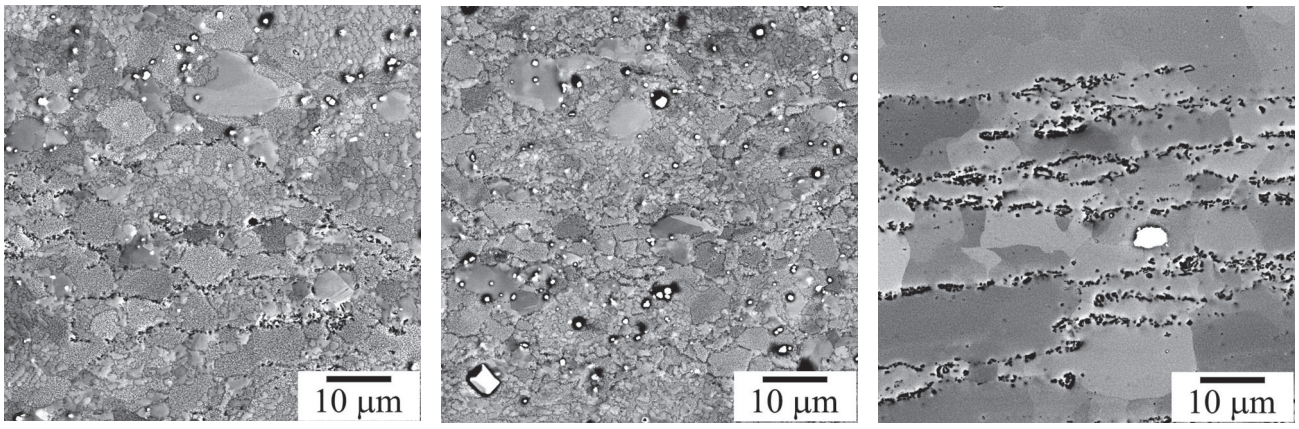

Fig. 3. BSE images of the samples compressed at T=1200°C (a), T=1225°C (b) and T=1240°C (c) ($\dot{\varepsilon}=10^{-3}$ s^{-1}, ε=65–70%).

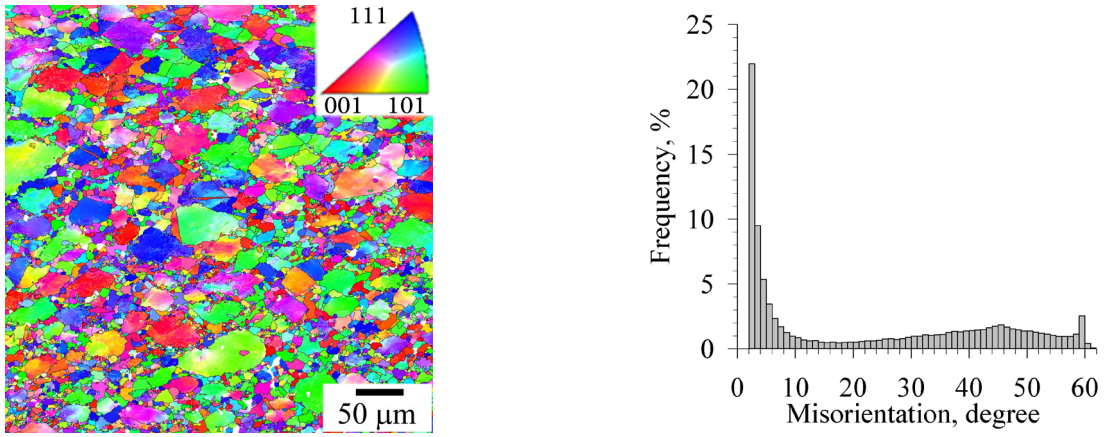

a b

Fig. 4. (Color online) Normal-direction electron backscatter diffraction (EBSD) (inverse-pole-figure) map (a) and the corresponding misorientation-angle distributions for grain/interphase boundaries (b) obtained from the central part of the sample deformed at T=1200°C ($\dot{\varepsilon}=10^{-2}$ s^{-1}, $\varepsilon=67.5\%$). The deformation axis is vertical, high- and low-angle grain/interphase boundaries are indicated by black and white lines, respectively.

grain/interphase boundaries obtained for the sample deformed at T=1200°C. One can see that the fraction of fine recrystallized γ grains is rather small and many coarse non-recrystallized γ grains are retained. They contain an increased dislocation density and sometimes annealing twins. The fraction of high-angle grain/interphase boundaries was found to be 50% (Fig. 4 b). Thus, recrystallization developed locally in all deformed samples with the cracks forming on the side surfaces of samples and the microcracks often forming along grain/interphase boundaries. The most probable reasons for the inefficiency of the isothermal hot deformation at T=1150–1240°C of the initial as-HIP'ed material are the chemical heterogeneity observed within some powder granules and the porosity of the initial material. To overcome these deficiencies, the as-HIP'ed material was subjected to preliminary homogenization. Note that the homogenization annealing for a shorter time (5–10 h) did not result in dissolution of γ + γ' eutectic areas and, therefore, the duration 15 h was used for homogenization.

Homogenization at 1220°C leads to some growth of γ grains. After annealing at 1220°C for 15 h the mean γ grain size increased from 27 to 42 μm. The homogenization was followed by slow cooling with a rate of 25°C/h to cause coarsening of the γ' phase [13]. Figure 5 represents the true stress-strain curves obtained as a result of compression tests of samples at 1200 and 1225°C in the initial HIP'ed and homogenized condition. One can see that homogenization resulted in a change of the curves. The flow stress first increases reaching maxima at a strain of $\varepsilon=5$–10% and then decreases that is typically associated with development of dynamic recrystallization. The samples compressed at 1200–1225°C after preliminary homogenization were free of any cracks on the side surfaces and microcracks. The reason why preliminary homogenization improved the hot workability and contributed to a more uniform development of recrystallization is not entirely clear. Preliminary homogenization and the temperature-strain rate conditions providing a good workability (T=1200–1225°C and $\dot{\varepsilon}=10^{-2}$ s^{-1}) were used for hot working of the superalloy billets under quasi-isothermal conditions.

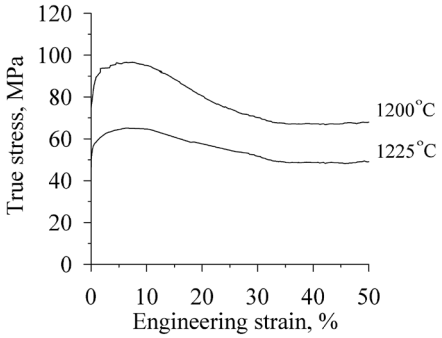

Fig. 5. The true stress-strain curves obtained as a result of compression tests of samples subjected to preliminary homogenization at 1220°C (15 h) ($\dot{\varepsilon}=10^{-2}$ s^{-1}).

3.3. Hot working and tensile properties

As was earlier shown for another heavily alloyed nickel-based superalloy [13,14], the fractional forging with intermediate recrystallization annealings contributed to a uniform development of recrystallization. In the present work, three-stage forging at 1225–1200°C with intermediate recrystallization annealings at 1200°C was applied to produce fine-grained workpieces. As a result, sound forgings with an approximate size of ∅80×10 mm free of any cracks were obtained. Figure 6 shows the macrostructure of the forged workpieces. It is near completely matte and uniform. Figure 7 represents the BSE image and EBSD map obtained from the central part of the forged workpiece. The obtained microstructure is near fully recrystallized and fine-grained with a γ grain size in the range of 5–20 μm. The size of non-recrystallized γ grains was about 50 μm. The fraction of primary γ' phase having a size of 1–8 μm is about 20%. The forged workpieces were subjected to solid solution treatment followed by cooling in air and ageing or only to ageing. The solution treatment was carried out at 1200–1210°C because a fast γ grain growth occurred during solution treatment at higher temperatures (1220–1230°C). The heat treated material retained the fine-grained structure ($d\leq$10–15 μm) and the fraction of primary γ' phase and led to formation of dispersed secondary γ'.

Fig. 6. (Color online) Macrostructures obtained in the workpieces of the PM Ni-16(Al, Ti, Nb, Ta)-30(Cr, Co, Mo, Hf, W, Re) superalloy after homogenization and three-stage forging at 1225–1200°C with intermediate recrystallization annealings at 1200°C.

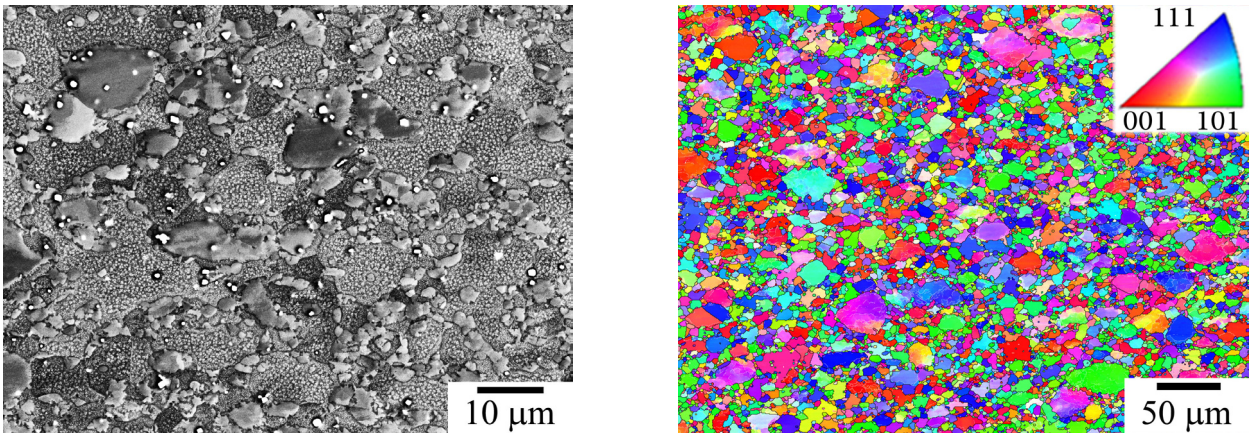

a b

Fig. 7. (Color online) BSE image (a) and normal-direction EBSD map (b) obtained from the central part of the workpiece after homogenization and three-stage forging at 1225–1200°C with intermediate annealings at 1200°C ($\dot{\varepsilon}=10^{-2}$ s^{-1}, $\varepsilon=72\%$). The forging axis is vertical, high- and low-angle grain/interphase boundaries are indicated by black and white lines, respectively (b).

The specimens for tensile testing were prepared from the fine-grained and heat treated forgings of the superalloy. The following tensile properties were obtained after homogenization, three-stage forging with intermediate annealings followed by solid solution treatment and ageing or only by ageing: the ultimate tensile strength UTS = 1757 ± 40 MPa, the yield strength YS = 1080 ± 40 MPa and elongation to fracture El = 16.5 ± 2% at room temperature; UTS = 1210 ± 40 MPa, YS = 1100 ± 40 MPa and El = (2.2 – 5.1) ± 0.4% at 750°C.

4. Conclusions

The novel PM nickel-based superalloy Ni-16(Al, Ti, Nb, Ta)-30(Cr, Co, Mo, Hf, W, Re) (wt.%) has been studied in the present work. The conclusions are as follows:

- in the as-HIP'ed condition the superalloy contained pores and sometimes non-equilibrium eutectics that decreased the hot workability and impeded the formation of a homogeneous recrystallized and fine-grained structure by hot working;

- preliminary homogenization of the as-HIP'ed material at subsolvus temperature improved the hot workability and promoted the formation of a homogeneous recrystallized and fine-grained structure;

- the hot working and heat treatment were developed for the superalloy. In the fine-grained condition obtained via optimal hot working and heat treatment the obtained tensile properties were found to be comparable with the best properties reached in disc nickel-based superalloys.

Acknowledgements. The work was supported by the Ministry of Science and Higher Education of the Russian Federation according to the State Assignment of the IMSP RAS (No. AAAA-A17-117041310215-4). The work was performed using the facilities of the shared services center "Structural and Physical-Mechanical Studies of Materials" at the Institute for Metals Superplasticity Problems of Russian Academy of Sciences.

References

1. R.C. Reed. The superalloys: Fundamentals and Applications. Cambridge University Press (2006) 372 p. Crossref
2. J.R. Li, Z.G. Zhong, D.Z. Tang, S.Z. Liu, P. Wei, P.Y. Wei, Z.T. Wu, D. Huang, M. Han. Superalloys. 2000, 777 (2000). Crossref
3. R.A. MacKay, T.P. Gabb, A. Garg, R.B. Rogers, M.V. Nathal. Mater. Characterization. 70, 83 (2012). Crossref
4. P. Wollgramm, H. Buck, K. Neuking, A.B. Parsa, S. Schuwalow, J. Rogal, R. Drautz, G. Eggeler. Mater. Sci. Eng. A. 628, 382 (2015). Crossref
5. N. Sun, L. Zhang, Z. Li, A. Shan. Mater. Sci. Eng. A. 606, 175 (2014). Crossref

6. D.P. Mourer, E.S. Huron, D.G. Backman, K.R. Bain, P.L. Reynolds, J.J. Schirra, T.P. Gabb. Ni based superalloy and its use as gas turbine disks, shafts, and impellers. Patent EP № 1195446 A1. 04 October 2000.
7. D.P. Mourer, E.S. Huron, K.R. Bain, E.E. Montero, P.L. Reynolds, J.J. Schirra. Superalloy optimized for high-temperature performance in high-pressure turbine disks. Patent US № 6521175 B1. 18 February 2003.
8. E.N. Kablov, B.S. Lomberg, L.S. Markina, S.V. Ovsepjan, E.N. Limonova, M.M. Bakradze, E.B. Chabina. Nickel-base heat-resistant deformable alloy and article made of this alloy. Patent RU № 2280091 C1. 21 December 2004. (in Russian)
9. G.S. Garibov, N.M. Grits, A.A. Inozemtsev, A.V. Vostrikov, E.A. Fedorenko, I.L. Andrejchenko, G.I. Zubarev, D.A. Karjagin. Refractory powder nickel-based alloy. Patent RU № 2410457 C1. 23 October 2009. (in Russian)
10. R.V. Khramin, M.N. Burov, A.V. Logunov, D.V. Danilov, I.A. Leshchenko, S.A. Zavodov, A.M. Mikhailov, M.A. Mikhailov, Sh.Kh. Mukhtarov, R.R. Mulyukov. Deformable nickel-based heat-resistant alloy. Patent RU № 2695097. 19 July 2019. (in Russian)
11. A. Mottura, R.C. Reed. MATEC Web of Conferences. 14, 01001 (2014). Crossref
12. Y.J. Wang, C.Y. Wang. Mater. Sci. Eng. A. 490, 242 (2008). Crossref
13. V. Imayev, S. Mukhtarov, K. Mukhtarova, A. Ganeev, R. Shakhov, N. Parkhimovich, A. Logunov. Metals. 10 (12), 1606 (2020). Crossref
14. V.M. Imayev, Sh.Kh. Mukhtarov, A.V. Logunov, A.A. Ganeev, R.V. Shakhov, R.M. Imayev. Letters on Materials. 9 (2), 249 (2019). (in Russian) Crossref
15. E.N. Kablov, N.V. Moiseev, B.S. Lomberg, M.M. Bakradze, B.R. Nekrasov, S.V. Vydumkina, A.V. Skugorev. Method for production of heat-resistant nickel alloys. Patent RU № 2661524 C1. 17 July 2018. (in Russian)
16. W. Guo, J. Wu, F. Zhang, M. Zhao. J. Iron Steel Res. Int. 13, 65 (2006). Crossref
17. Y. Tao, J. Jia, J.Liu. J. Iron Steel Res. Int. 17 (9), 73 (2010). Crossref
18. J.B. Moore, J. Tequesta, R.L. Athey. Fabrication method for the high temperature alloys. Patent US № 1970/3519503. 07 July 1970.
19. E.L. Raymond, R.G. Menzies, T.O. Dyer, B.A. Link, R.F. Halter, M.E. Mechley, F.M. Visalli, S.K. Srivatsa. Quasi-Isothermal forging of a nickel-base superalloy. Patent EP № 1416062 A2. 06 May 2004.
20. A.A. Ganeev, V.A. Valitov, F.Z. Utyashev, V.M. Imayev. Phys. Metals Metallogr. 120, 410 (2019). Crossref
21. O.Kh. Fatkullin, V.I. Eremenko, O.N. Vlasova, N.M. Grits. Technology of Light Alloys. 5 – 6, 149 (2001). (in Russian)
22. S.A. Kononov, A.S. Perevozov, B.A. Kolachev. Russ. Metall. 5, 415 (2007). Crossref
23. A.G. Beresnev, A.V. Logunov, A.I. Logacheva. Vestnik MAI. 15 (3), 17 (2008). (in Russian)